Signal processing for MIMO radars: Detection under Gaussian and non-Gaussian environments and application to STAP

CHONG Chin Yuan

Thesis Director: Marc LESTURGIE (ONERA/SONDRA)
Supervisor: Frédéric PASCAL (SONDRA)

18th Nov 2011

Outline

Outline

- Overview of MIMO Radars
- MIMO Detectors
- Application: STAP
- Conclusions

What is a MIMO Radar?

Multiple-Input Multiple-Output $\Rightarrow$ DIVERSITY!!

Multiple-Input (MI)

- Transmit waveform diversity
- Transmit spatial diversity

Multiple-Output (MO)

- Receive spatial diversity

Statistical MIMO Radars Tx and Rx antennas are all widely separated

Coherent MIMO Radars Tx and Rx antennas are closely spaced to form a single Tx and Rx subarray

Hybrid MIMO Radars Widely separated Tx and Rx subarrays, each containing one or more antennas

Statistical MIMO Radar

- Widely-separated antennas ⇒ spatial diversity
  - Independent aspects of target → overcome fluctuations of target RCS, esp in case of distributed complex targets ⇒ diversity gain
  - Moving targets have different LOS speeds for different antennas ⇒ geometry gain
  - Possibility of target characterization and classification
- Without waveform diversity, transmit spatial diversity cannot be exploited at the receive end
- LPI advantage due to isotropic radiation
- Non-coherent processing → no coherent gain BUT no phase synchronization needed
- Applications: Detection, SAR

Statistical MIMO Radar Vs Multistatic Radar

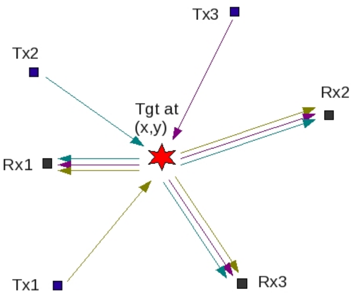

Statistical MIMO

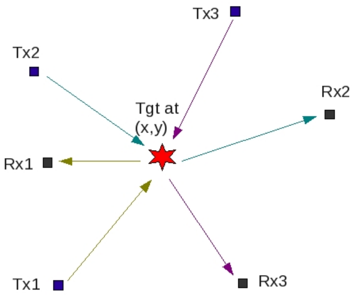

Multistatic radar

Joint processing of all antennas
→ Centralized detection strategy

Each rx antenna receives only signals from corresponding tx antenna
→ Decentralized detection strategy

Coherent MIMO Radar

- No spatial diversity. Diversity comes only from waveforms
- Transmit and receive subarray can be sparse $\rightarrow$ improve resolution but can cause grating lobes
- Improved direction-finding capabilities at expense of diversity
- Improved parameter estimation (identifiability, resolution, etc)
- Applications: Direction-finding, STAP/GMTI

Coherent MIMO Radar Vs Phased-Array Radar

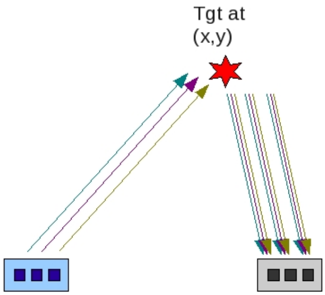

Coherent MIMO

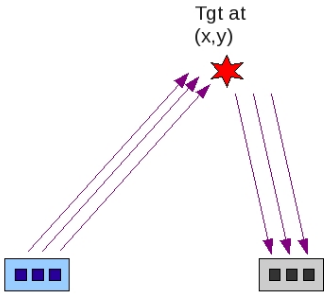

Phased array

Different waveforms are transmitted from each closely-spaced transmit antenna

Only one transmit antenna or single waveform is transmitted from all closely-spaced transmit antennas

Configuration overview

SISO	SIMO
MISO	MIMO

Configuration overview

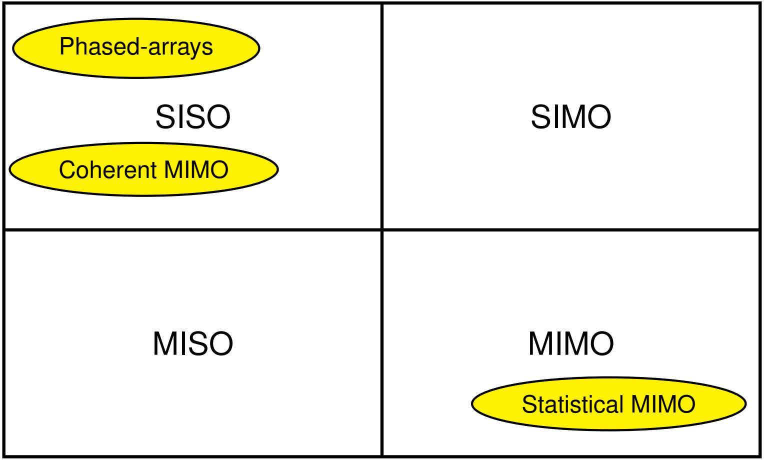

Configuration overview

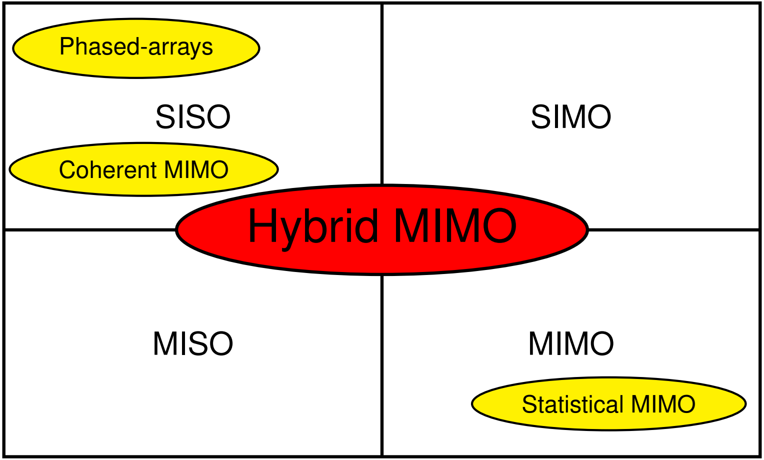

Hybrid Configuration

General case with few assumptions!

Effective number of subarrays K_e:

- $K_e \geq \tilde{N} + \tilde{M}$ if $\tilde{N}, \tilde{M} > 1$ (diversity gain)
- Big K_e robust against target fluctuations $\rightarrow$ surveillance
- Small K_e better gain $\rightarrow$ direction finding

Config	$\tilde{N}$	N_n	$\tilde{M}$	M_m
SISO	1	≥ 1	1	≥ 1
SIMO	1	≥ 1	> 1	≥ 1
MISO	> 1	≥ 1	1	≥ 1
MIMO	> 1	≥ 1	> 1	≥ 1

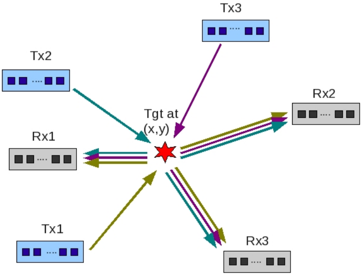

Effective number of elements N_e:

- $N_e \geq N_{rx} + N_{tx}$ if $N_{rx}, N_{tx} > 1$ (diversity gain)
- Maximum N_e if $N_{rx} = N_{tx}$, irregardless number of subarrays
- Better to have more N_{rx} for SIR gain

Outline

Signal Model (1/2)

Received signal after range matched-filtering:

$$\mathbf{y} = \mathbf{P}\boldsymbol{\alpha} + \mathbf{z},$$

where the vectors $\mathbf{y}$, $\boldsymbol{\alpha}$ and $\mathbf{z}$ are the concatenations of all the received signals, target RCS and clutter returns, respectively:

$$\mathbf{y} = \begin{bmatrix} \mathbf{y}_{1,1} \\ \vdots \\ \mathbf{y}_{\tilde{M},\tilde{N}} \end{bmatrix} \quad \boldsymbol{\alpha} = \begin{bmatrix} \alpha_{1,1} \\ \vdots \\ \alpha_{\tilde{M},\tilde{N}} \end{bmatrix} \quad \mathbf{z} = \begin{bmatrix} \mathbf{z}_{1,1} \\ \vdots \\ \mathbf{z}_{\tilde{M},\tilde{N}} \end{bmatrix}$$

$\mathbf{P}$ is the $(\sum_{m,n=1}^{\tilde{M},\tilde{N}} M_m N_n)$ x $\tilde{M}\tilde{N}$ matrix containing all the steering vectors:

$$\mathbf{P} = \begin{bmatrix} \mathbf{p}_{1,1} & & \mathbf{0} \\ & \ddots & \\ \mathbf{0} & & \mathbf{p}_{\tilde{M},\tilde{N}} \end{bmatrix}$$

Signal Model (2/2)

Steering vector $\mathbf{p}_{m,n}$

$\mathbf{p}_{m,n}$ can be generalized to include different parameters, e.g. Doppler

Interference $\mathbf{z}_{m,n}$

- $\mathbf{z} \sim \mathcal{CN}(\mathbf{0}, \mathbf{M})$: covariance matrix of each $\mathbf{z}_i$ is given by $\mathbf{M}_{ii}$, inter-correlation matrix between $\mathbf{z}_i$ and $\mathbf{z}_j$ is given by $\mathbf{M}_{ij}$
- Takes into account correlation arising from insufficient spacing between subarrays and non-orthogonal waveforms

MIMO Gaussian Detector

Consider the following hypothesis test:

$$\begin{cases} \mathrm{H}_0 : & \mathbf{y} = \mathbf{z} & \text{interference only} \\ \mathrm{H}_1 : & \mathbf{y} = \mathbf{P}\alpha + \mathbf{z} & \text{target and interference} \end{cases}$$

Based on Maximum-Likelihood theory, the MIMO detector has been derived to be:

$$\boxed{\Lambda(\mathbf{y}) = \mathbf{y}^\dagger \mathbf{M}^{-1}\mathbf{P}(\mathbf{P}^\dagger \mathbf{M}^{-1}\mathbf{P})^{-1}\mathbf{P}^\dagger \mathbf{M}^{-1}\mathbf{y} \underset{\mathrm{H}_0}{\overset{\mathrm{H}_1}{\gtrless}} \lambda.}$$

Equivalent to multi-dimensional version of OGD and can be considered as a generalized version of MIMO OGD as it becomes MIMO OGD when the subarrays are non-correlated.

$$\text{MIMO OGD:} \quad \sum_{m,n} \frac{|\mathbf{p}_{m,n}^\dagger \mathbf{M}_{m,n}^{-1}\mathbf{y}_{m,n}|^2}{\mathbf{p}_{m,n}^\dagger \mathbf{M}_{m,n}^{-1}\mathbf{p}_{m,n}}$$

Statistical Properties

$$\Lambda(\mathbf{y}) \overset{d}{=} \begin{cases} \mathrm{H}_0 : & \frac{1}{2}\chi^2_{2K_e}(0) \\ \mathrm{H}_1 : & \frac{1}{2}\chi^2_{2K_e}(2\alpha^\dagger \mathbf{P}^\dagger \mathbf{M}^{-1}\mathbf{P}\alpha) \end{cases}$$

- Non-centrality parameter is equal to $2\alpha^\dagger \mathbf{P}^\dagger \mathbf{M}^{-1}\mathbf{P}\alpha$
- Detector is **M**-CFAR as distribution under H_0 does not depend on correlation between subarrays
- Requirement of independence between subarrays can be relaxed for some applications, e.g. regulation of false alarms

Simulation Configurations

Total number of antennas, $N_p = 13$

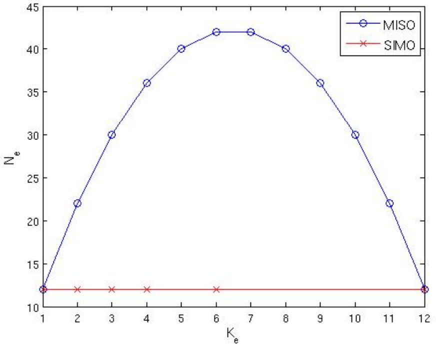

Variation of N_e with K_e for MISO and SIMO cases

SIMO Case

One single transmit element and K_e receive subarray with $\frac{N_p-1}{K_e}$ elements

MISO Case

K_e transmit elements and one single receive subarray with $N_p - K_e$ elements

Detection Performance

SIMO case

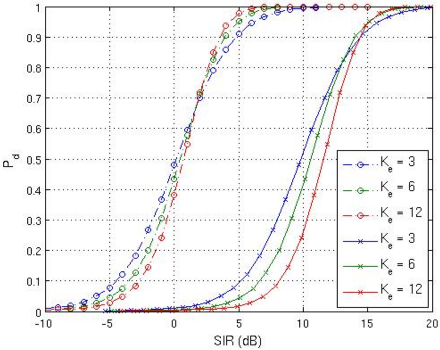

MISO case

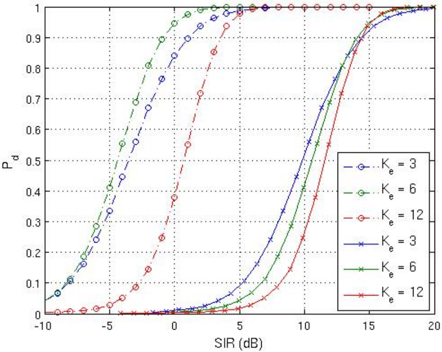

P_d against SIR_{pre} (dash-dotted lines) and SIR_{post} (solid lines). $P_{fa} = 10^{-3}$
Fluctuating target modeled similar to Swerling I target

Detection Performance

SIMO case

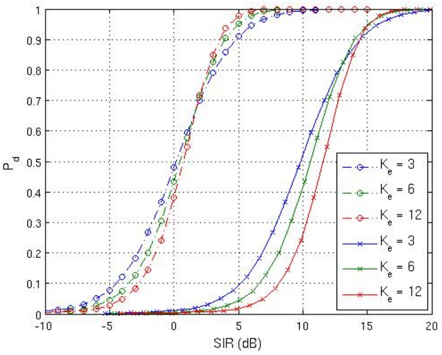

- N_e remains the same → same SIR gain
- Threshold higher for higher DoF → causes performance to degrade
- But higher DoF more robust to target fluctuations
- High P_d → better with large K_e and small K_e better at low P_d

Detection Performance

- Poor performance for $K_e = 12$ due to high threshold and no SIR gain
- $K_e = 6$ has high SIR gain to offset increase of threshold with DoF
- $K_e = 6$ is more robust to target fluctuations $\rightarrow$ big advantage over $K_e = 3$ at high P_d

MISO case

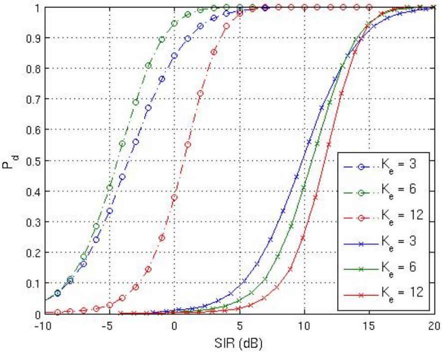

Adaptive Version

Based on Kelly's Test, the optimum adaptive detector is derived to be:

$$\boxed{\hat{\Lambda}(\mathbf{y}) = \frac{\mathbf{y}^\dagger \widehat{\mathbf{M}}^{-1} \mathbf{P} (\mathbf{P}^\dagger \widehat{\mathbf{M}}^{-1} \mathbf{P})^{-1} \mathbf{P}^\dagger \widehat{\mathbf{M}}^{-1} \mathbf{y}}{N_s + \mathbf{y}^\dagger \widehat{\mathbf{M}}^{-1} \mathbf{y}}}$$

where $\widehat{\mathbf{M}}$ is the Sample Covariance Matrix of $\mathbf{M}$ and is given by:

$$\widehat{\mathbf{M}} = \frac{1}{N_s} \sum_{l=1}^{Ns} \mathbf{c}(l)\mathbf{c}(l)^\dagger .$$

$\mathbf{c}(l)$ are target-free secondary data (i.i.d) and N_s is the number of secondary data.

Statistical Properties

$$\hat{\Lambda}(\mathbf{y}) \overset{d}{=} \begin{cases} \mathrm{H}_0: & \beta_{K_e, N_s - N_e + 1}(0), \\ \mathrm{H}_1: & \beta_{K_e, N_s - N_e + 1}(\gamma), \end{cases}$$

where $\gamma = 2\alpha^\dagger \mathbf{P}^\dagger \mathbf{M}^{-1} \mathbf{P} \alpha \cdot l_f$ $\quad l_f \sim \beta_{N_s - N_e + K_e + 1, N_e - K_e}$

Loss factor l_f

- l_f is loss factor on SIR due to estimation of covariance matrix
- If only 1 effective element per subarray i.e. $N_e = K_e$, $l_f = 1$

Loss factor l_f

Mean or expected value of l_f is given by:

$$E(l_f) = \frac{N_s - N_e + K_e + 1}{N_s + 1}.$$

- For fixed N_s, better with smaller N_e and bigger K_e to reduce loss
- To limit loss to 3 dB, i.e. $E(l_f > 0.5)$ $\Rightarrow N_s > 2N_e - 2K_e - 1$, providing $N_s \geq N_e$ so that SCM is of full rank
- For phased-arrays ($K_e = 1$) $\Rightarrow N_s > 2N_e - 3$ $\Rightarrow$ Reed-Mallet-Brennan's rule

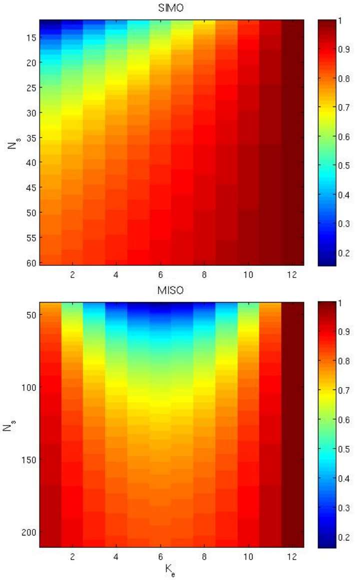

Detection Performance

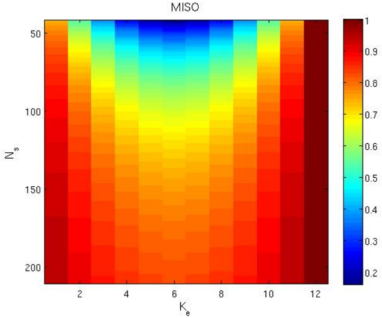

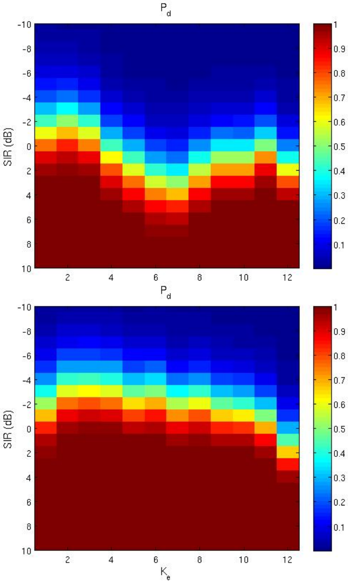

Detection Performance

Few secondary data → loss in SIR
due to estimation of covariance matrix
depends greatly on K_e

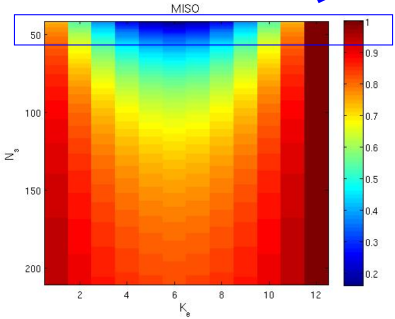

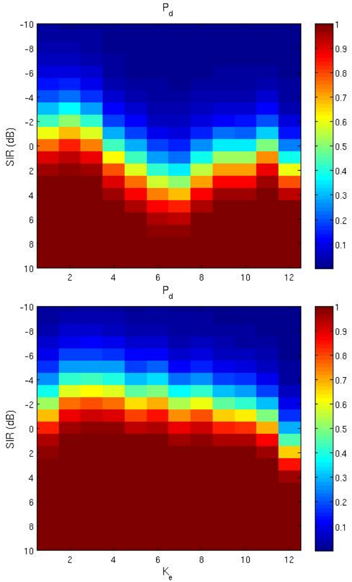

Detection Performance

Few secondary data → loss in SIR due to estimation of covariance matrix depends greatly on K_e

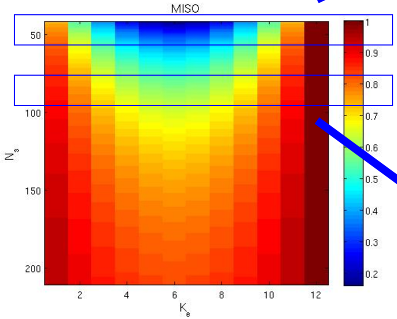

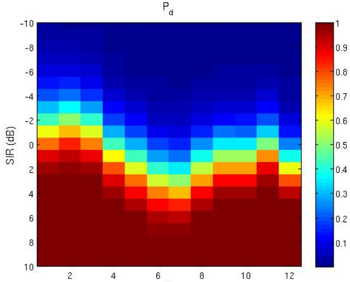

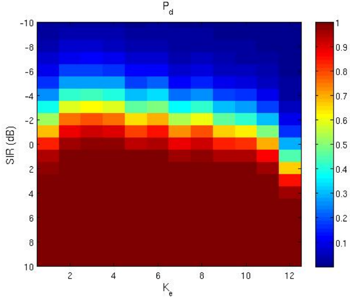

Enough secondary data → SIR loss insignificant → more important to increase processing gain

Why non-Gaussian clutter?

- As resolution improves, resolution cell becomes smaller $\rightarrow$ fewer scatterers in each cell $\rightarrow$ CLT no longer applies $\rightarrow$ non-Gaussian clutter
- Widely separated subarrays $\rightarrow$ different aspects of each resolution cell $\rightarrow$ non-Gaussian clutter
- Experimental radar clutter measurements $\rightarrow$ fit non-Gaussian statistical models

Subarrays are assumed to be INDEPENDENT!

Clutter Model

$\mathbf{z}_{m,n}$ is modeled by Spherically Invariant Random Vector (SIRV):

$$\mathbf{z}_{m,n} = \sqrt{\tau_{m,n}}\, \mathbf{x}_{m,n}$$

- *speckle* - a Gaussian random process $\mathbf{x}_{m,n} \sim \mathcal{CN}(\mathbf{0}, \mathbf{M}_{m,n})$ which models temporal fluctuations of clutter
- *texture* - square-root of a non-negative random variable $\tau_{m,n}$ which models spatial fluctuations of clutter power

- Models different non-Gaussian clutter depending on chosen texture
- Includes Gaussian clutter as special case where texture is a constant
- Gaussian kernel $\rightarrow$ classical ML methods for parameter estimation

MIMO Non-Gaussian Detector

Based on the GLRT-LQ test and independent subarray assumption, the MIMO GLRT-LQ test is derived to be:

$$\boxed{\prod_{m,n}\left[1-\frac{|\mathbf{p}_{m,n}^{\dagger}\mathbf{M}_{m,n}^{-1}\mathbf{y}_{m,n}|^2}{(\mathbf{p}_{m,n}^{\dagger}\mathbf{M}_{m,n}^{-1}\mathbf{p}_{m,n})(\mathbf{y}_{m,n}^{\dagger}\mathbf{M}_{m,n}^{-1}\mathbf{y}_{m,n})}\right]^{-M_m N_n}\underset{H_0}{\overset{H_1}{\gtrless}}\eta}$$

The GLRT-LQ detector is homogeneous in terms of $\mathbf{p}_{m,n}$, $\mathbf{M}_{m,n}$ and $\mathbf{y}_{m,n}$ such that it is invariant to data scaling $\Rightarrow$ detector is texture-CFAR

Theoretical Performance

Theorem

Given a MIMO radar system containing K_e subarrays with L elements each, the probability of false alarm of the MIMO GLRT-LQ detector is given by:

$$P_{fa} = \lambda^{-L+1} \sum_{k=0}^{K_e - 1} \frac{(L-1)^k}{k!} (\ln \lambda)^k.$$

where $\lambda = \sqrt[L]{\eta}$.

- P_{fa} depends only on K_e and L and not on the clutter parameters $\Rightarrow$ detector is texture-CFAR.
- Does not depend on the covariance matrices which can be different for each subarray.
- Useful for the analysis of detection performance.

Simulation Parameters

$\tilde{M}$	$\tilde{N}$	M_m	N_n	$K_e = \tilde{M}\tilde{N}$	$N_e = M_m N_n$	$\sigma^2 = E(\tau)$
3	2	4	3	6	12	1

Experimental radar clutter measurements:
texture follows Gamma (K-distributed clutter) or Weibull distribution

Texture distribution	a	b
1. Gamma	2	$\frac{\sigma^2}{a} = 0.5$
2. Gamma	0.5	$\frac{\sigma^2}{a} = 2$
1. Weibull	$\frac{\sigma^2}{\Gamma(1+\frac{1}{b})} = 1.1233$	1.763
2. Weibull	$\frac{\sigma^2}{\Gamma(1+\frac{1}{b})} = 0.7418$	0.658

Gaussian clutter as comparison

Clutter power

Gaussian clutter

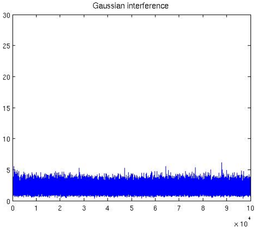

K-distributed clutter

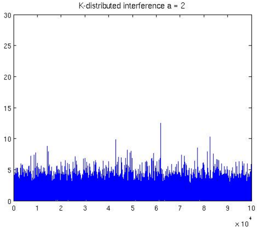

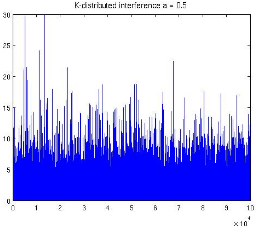

Weibull-textured clutter

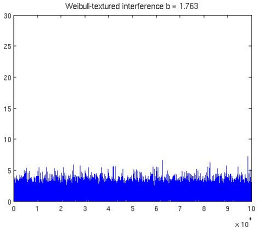

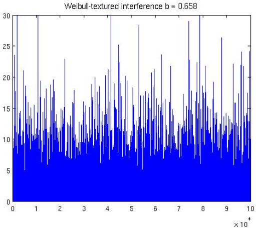

Texture-CFAR property of MIMO Non-Gaussian Detector

Same threshold for same P_{fa} irregardless of clutter texture!
Good agreement between theory and simulation!

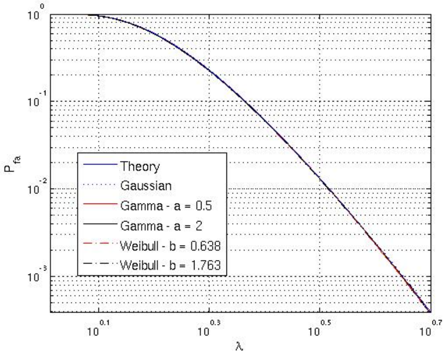

Detection Performance under K-distributed Clutter

$a = 0.5 \Rightarrow$ impulsive clutter

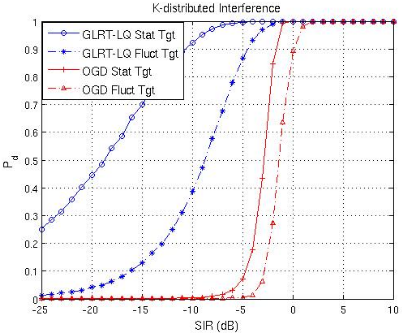

$a = 2 \Rightarrow$ similar to Gaussian clutter

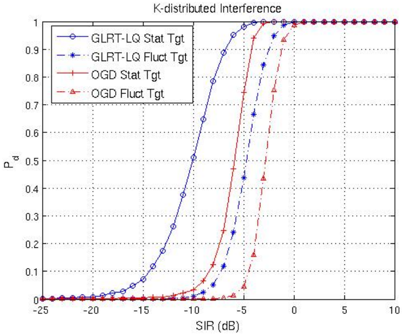

Stationary target model (same SIR for all subarrays) as comparison

Detection Performance under K-distributed Clutter

- Clutter similar to that of Gaussian clutter
- MIMO GLRT-LQ works better than MIMO OGD especially when SIR is low
- MIMO GLRT-LQ more affected by fluctuations of target but still better than MIMO OGD

$a = 2 \Rightarrow$ similar to Gaussian clutter

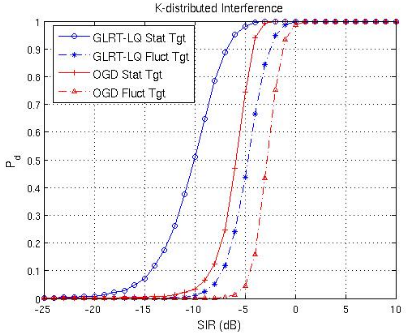

Detection Performance under K-distributed Clutter

$a = 0.5 \Rightarrow$ impulsive clutter

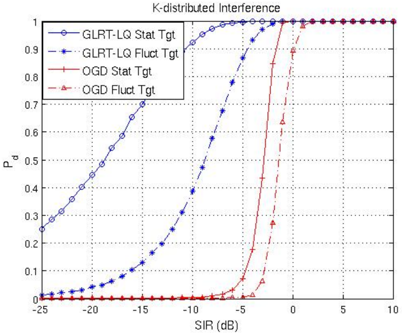

- Clutter is impulsive
- MIMO GLRT-LQ works MUCH better than MIMO OGD due to normalizing term which takes into account variation of clutter power
- MIMO GLRT-LQ more affected by fluctuations of target but still better than MIMO OGD

Detection Performance under Gaussian Clutter

MIMO GLRT-LQ is slightly worse than MIMO OGD under Gaussian clutter but more robust as it works under different types of clutter!

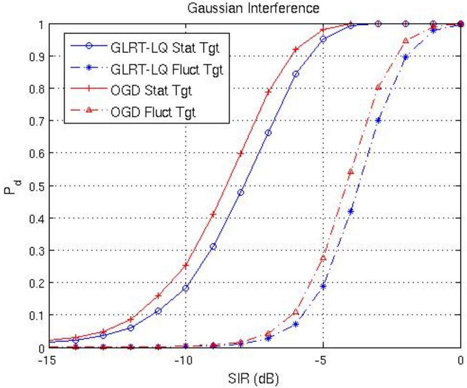

Adaptive Non-Gaussian MIMO Detector

The adaptive detector is obtained by replacing $\mathbf{M}_{m,n}$ by its estimate $\widehat{\mathbf{M}}_{m,n}$:

$$\boxed{\prod_{m,n}\left[1-\frac{|\mathbf{p}_{m,n}^{\dagger}\widehat{\mathbf{M}}_{m,n}^{-1}\mathbf{y}_{m,n}|^2}{(\mathbf{p}_{m,n}^{\dagger}\widehat{\mathbf{M}}_{m,n}^{-1}\mathbf{p}_{m,n})(\mathbf{y}_{m,n}^{\dagger}\widehat{\mathbf{M}}_{m,n}^{-1}\mathbf{y}_{m,n})}\right]^{-M_mN_n}}$$

Under non-Gaussian clutter, the SCM is no longer the ML estimate
$\Rightarrow$ use Fixed Point Estimate given by:

$$\widehat{\mathbf{M}}_{FP}=\frac{M_mN_n}{N_{s\,m,n}}\sum_{l=1}^{N_{s\,m,n}}\frac{\mathbf{y}_{m,n}(l)\mathbf{y}_{m,n}^{\dagger}(l)}{\mathbf{y}_{m,n}^{\dagger}(l)\widehat{\mathbf{M}}_{FP}^{-1}\mathbf{y}_{m,n}(l)}$$

- Can be solved by iterative algorithm which tends to $\widehat{\mathbf{M}}_{FP}$ irregardless of the initial matrix
- Asymptotic distribution of $\widehat{\mathbf{M}}_{FP}$ is the same as that of the SCM with $\frac{M_mN_n}{M_mN_n+1}N_{s\,m,n}$ secondary data under *Gaussian* clutter

Detection Performance under K-distributed Clutter

$a = 0.5 \Rightarrow$ impulsive clutter

$a = 2 \Rightarrow$ similar to Gaussian clutter

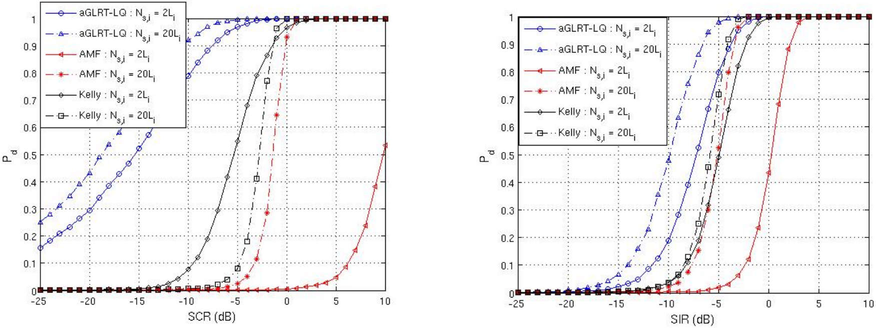

Estimation of covariance matrix:

MIMO aGLRT-LQ $\rightarrow$ FPE (10 iterations) while MIMO AMF, MIMO Kelly's Test $\rightarrow$ SCM

Detection Performance under K-distributed Clutter

$a = 2 \Rightarrow$ similar to Gaussian clutter

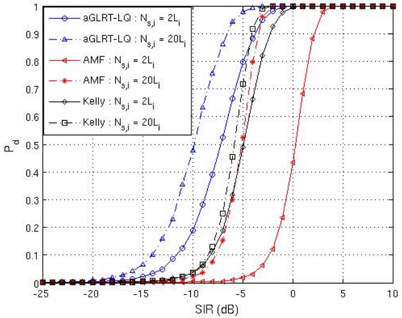

- Clutter is similar to Gaussian case
- MIMO aGLRT-LQ better than MIMO AMF and MIMO Kelly's Test
- MIMO AMF more affected by estimation of covariance matrix since SCM is NOT ML under non-Gaussian clutter

MIMO AMF: $$\sum_{m,n} \frac{|\mathbf{p}_{m,n}^{\dagger} \widehat{\mathbf{M}}_{m,n}^{-1} \mathbf{y}_{m,n}|^2}{\mathbf{p}_{m,n}^{\dagger} \widehat{\mathbf{M}}_{m,n}^{-1} \mathbf{p}_{m,n}}$$

MIMO Kelly's Test: $$\prod_{m,n} \left[1 - \frac{|\mathbf{p}_{m,n}^{\dagger} \widehat{\mathbf{M}}_{SCM,m,n}^{-1} \mathbf{y}_{m,n}|^2}{(\mathbf{p}_{m,n}^{\dagger} \widehat{\mathbf{M}}_{SCM,m,n}^{-1} \mathbf{p}_{m,n})(N_{s\,m,n} + \mathbf{y}_{m,n}^{\dagger} \widehat{\mathbf{M}}_{SCM,m,n}^{-1} \mathbf{y}_{m,n})} \right]^{-N_{s\,m,n}}$$

Detection Performance under K-distributed Clutter

$a = 0.5 \Rightarrow$ impulsive clutter

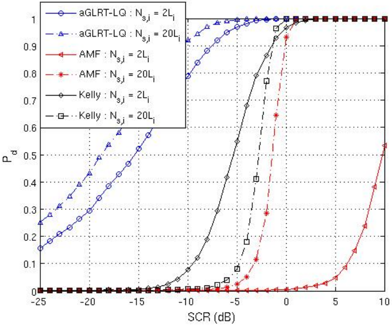

- Clutter is impulsive
- MIMO aGLRT-LQ is much better than MIMO AMF and MIMO Kelly's Test as it can take into account variations of clutter power
- MIMO AMF and MIMO Kelly's Test are affected by the estimation of covariance matrix
- MIMO Kelly's Test more similar to MIMO aGLRT-LQ when $N_{s m,n}$ is small while it is nearer to MIMO AMF when $N_{s m,n}$ is large

Adaptive Version - Gaussian Clutter

- When $N_{s m,n} = 20N_e$, MIMO aGLRT-LQ is slightly worse than MIMO AMF, as in non-adaptive case
- MIMO aGLRT-LQ is slightly better than MIMO AMF when $N_{s m,n} = 2N_e$!
  - Under Gaussian clutter, MIMO AMF expected to perform worse than MIMO Kelly's Test as $\mathbf{y}_{m,n}$ is not used in derivation of detector
  - For large $N_{s m,n}$, MIMO Kelly's Test $\approx$ MIMO AMF BUT normalizing term is no longer negligible for small $N_{s m,n}$ and MIMO Kelly's Test $\rightarrow$ MIMO aGLRT-LQ

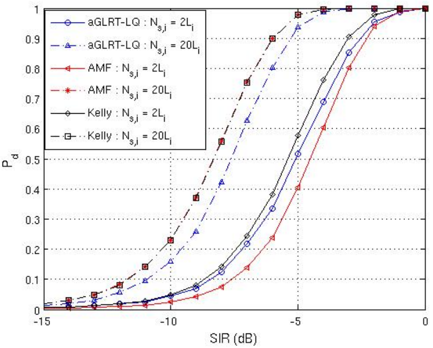

Outline

Motivation

Why use Space-Time Adaptive Processing (STAP)?

- Main application: Ground Moving Target Indication (GMTI)
- Slow moving target in strong clutter background
- Moving platform causes angle-Doppler dependence of clutter → enables slow target detection
- Joint processing of temporal and spatial dimensions → better suppression of clutter

Why use Multi-Input Multi-Output (MIMO) techniques?

- Increase angular resolution → further increase separation between clutter and target → more efficient clutter suppression and lower Minimum Detectable Velocity (MDV)
- More degrees of freedom for clutter cancellation

SISO-STAP Signal Model (1/2)

- Only one transmit and one receive subarray
- Transmit and receive are co-located $\rightarrow$ all elements see the same target RCS
- Different waveforms transmitted s.t. received signal can be separated

Received signal after range matched-filtering:

$$\mathbf{y} = ae^{j\phi}\,\mathbf{p}(\theta, f_d) + \mathbf{c} + \mathbf{n}$$

where $ae^{j\phi}$ is the complex target RCS
$\mathbf{p}(\theta, f_d)$ is the space-time steering vector,
θ is the receive/transmit angle and f_d is the relative Doppler frequency,
$\mathbf{c} \sim \mathcal{CN}(\mathbf{0}, \mathbf{M}_c)$ is the clutter vector and $\mathbf{M}_c$ is the clutter covariance matrix,
$\mathbf{n} \sim \mathcal{CN}(\mathbf{0}, \sigma^2\mathbf{I})$ is the noise vector and σ^2 is the noise power.

SISO-STAP Signal Model (2/2)

The steering vector **p** can also be expressed as:

$$\mathbf{p}(\theta, f_d) = \mathbf{a}(\theta) \otimes \mathbf{b}(\theta) \otimes \mathbf{v}(f_d).$$

Note that $\mathbf{p}(\theta, f_d) = \mathbf{a}(\theta) \otimes \mathbf{v}(f_d)$ for classical STAP.

The receive, transmit and Doppler steering vectors are as follows:

$$\begin{aligned}
\mathbf{a}(\theta) &= [1 \ \cdots \ \exp(j2\pi \frac{(M-1)d_r}{\lambda} \sin\theta)]^T, \\
\mathbf{b}(\theta) &= [1 \ \cdots \ \exp(j2\pi \frac{(N-1)d_t}{\lambda} \sin\theta)]^T, \\
\mathbf{v}(f_d) &= [1 \ \cdots \ \exp(j2\pi (L-1)\, \mathrm{PRI} \cdot f_d)]^T,
\end{aligned}$$

where M, N are number of receive/transmit elements,
d_r, d_t are the inter-element spacing for the receive/transmit subarrays,
L is number of pulses and PRI is the Pulse Repetition Interval,
v is the platform velocity and λ is the wavelength of the radar.

Element Distribution Configurations (1/2)

Maximum N_e

Given a fixed N_p, the maximum possible effective number of elements is given by:

$$N_e^{max} = \begin{cases} \frac{N_p^2}{4} & N_p \text{ even} \\ \frac{N_p^2 - 1}{4} & N_p \text{ odd} \end{cases}$$

Maximum L_a

Given a fixed N_p, the maximum possible aperture size given critical sampling is:

$$L_a^{max} = \begin{cases} (\frac{{N_p}^2}{4} - 1)\frac{\lambda}{2} & N_p \text{ even} \\ (\frac{{N_p}^2 - 5}{4})\frac{\lambda}{2} & N_p \text{ odd} \end{cases}$$

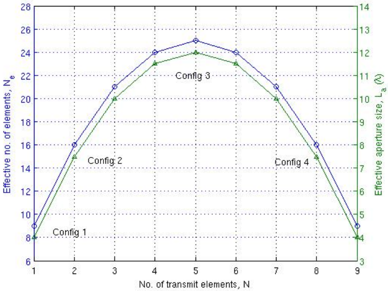

Config	N	M	N_e	L_a/λ
1	1	9	9	4
2	2	8	16	7.5
3	5	5	25	12
4	8	2	16	7.5

Element Distribution Configurations (2/2)

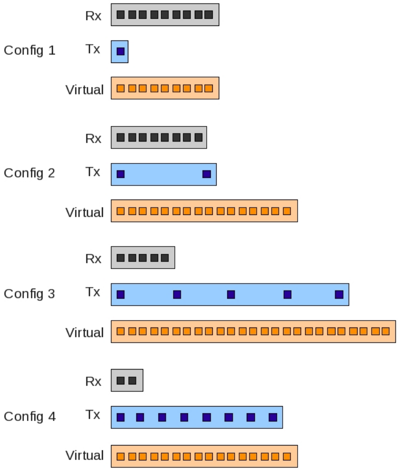

Generalized MIMO Brennan's Rule

Define α, β and γ as below:

$$\alpha = \frac{d_r}{\lambda/2}, \qquad \beta = \frac{2v\mathrm{PRI}}{\lambda/2}, \qquad \gamma = \frac{d_t}{\lambda/2}.$$

In the case where α, β and γ are integers, the rank of clutter covariance matrix is given by the number of distinct (integer) values N_d in:

$$m\alpha + n\gamma + l\beta \quad \forall \quad \begin{cases} m = 0, \dots, M-1 \\ n = 0, \dots, N-1 \\ l = 0, \dots, L-1. \end{cases}$$

- When α, β and γ are not integers, the rank of $\mathbf{M}_c$ is *approximated* by N_d.
- When $\alpha = 1$, i.e. $d_r = \lambda/2$, we obtain the MIMO extension of Brennan's Rule.
- If $\min(\alpha, \beta, \gamma) = 1$, then $N_d = (M-1)\alpha + (N-1)\gamma + (L-1)\beta + 1$.
- If α, γ and β are divisible by $\min(\alpha, \beta, \gamma)$, then $N_d = \frac{(M-1)\alpha + (N-1)\gamma + (L-1)\beta}{\min(\alpha,\beta,\gamma)} + 1$.

Synthetic Array

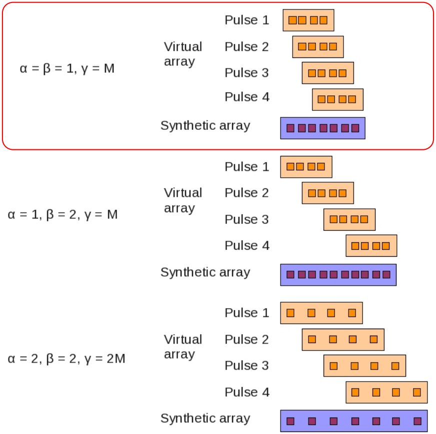

- $\beta = 1 \Rightarrow$ radar moves by one element spacing between pulses
  $L_{syn} = 3\lambda$ and $N_d = 7$

Synthetic Array

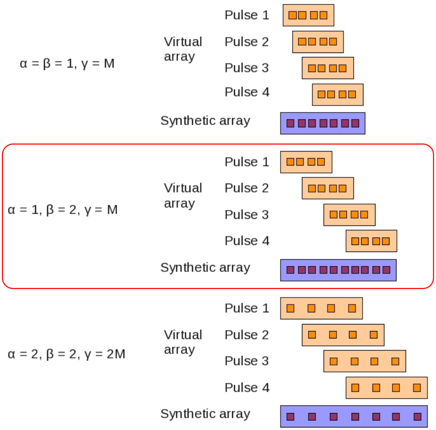

- $\beta = 2 \Rightarrow$ less overlap of array between pulses $\rightarrow$ increase in synthetic array size and improve resolution BUT clutter rank increases and ambiguities arise $L_{syn} = 4.5\lambda$ and $N_d = 10$

Synthetic Array

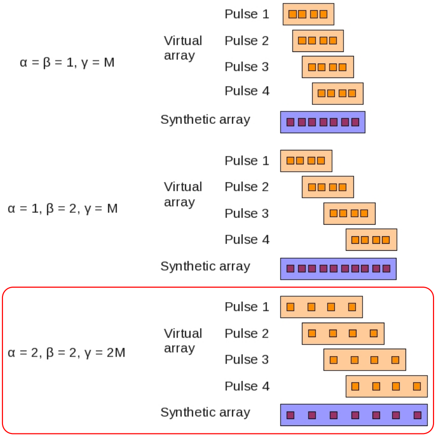

- $\beta = 2$ AND $\alpha = 2 \Rightarrow$ positions of elements from pulse to pulse are aligned $\rightarrow$ reduces clutter rank AND same ambiguities. Resolution improves further $L_{syn} = 6\lambda$ and $N_d = 7$

Element Spacing Configurations (1/2)

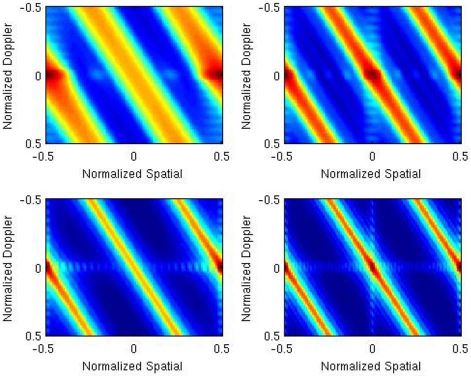

Config	α	γ	rank($\mathbf{M}_c$)
a	1	α	39
b	2	α	24
c	1	αM=5	55
d	2	αM=10	40

- Ambiguity in Doppler ($\beta = 2$)
- Spatial ambiguities added to reduce width of clutter ridges and clutter rank (Config b and d)
- Additional clutter ridges overlap existing ones $\rightarrow$ no increase in number of clutter ridges

Element Spacing Configurations (2/2)

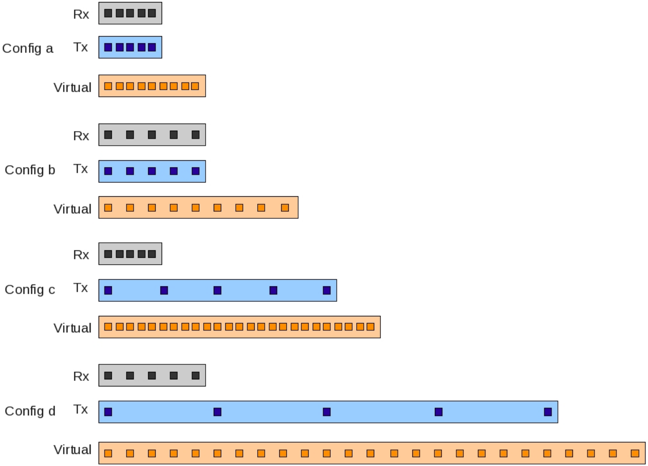

Cramér-Rao Bounds

Cramér-Rao bound (CRB)

Cramér-Rao bound (CRB) expresses a lower bound on the variance of estimators of a deterministic parameter. For $\mathbf{y} \sim \mathcal{CN}(\boldsymbol{\mu}(\boldsymbol{\Theta}), \mathbf{M}(\boldsymbol{\Theta}))$, the Fisher Information Matrix $\mathbf{J}$ is given by:

$$[\mathbf{J}(\boldsymbol{\Theta})]_{i,j} = \mathrm{tr}\left[\mathbf{M}(\boldsymbol{\Theta})^{-1}\frac{\partial \mathbf{M}(\boldsymbol{\Theta})}{\partial \Theta_i}\mathbf{M}(\boldsymbol{\Theta})^{-1}\frac{\partial \mathbf{M}(\boldsymbol{\Theta})}{\partial \Theta_j}\right] + 2\Re\left[\frac{\partial \boldsymbol{\mu}^{\dagger}(\boldsymbol{\Theta})}{\partial \Theta_i}\mathbf{M}(\boldsymbol{\Theta})^{-1}\frac{\partial \boldsymbol{\mu}(\boldsymbol{\Theta})}{\partial \Theta_j}\right]$$

Signal parameters to be estimated are:

$$\boldsymbol{\Theta} = [\ \boldsymbol{\Theta}_S \ \ \boldsymbol{\Theta}_I\ ].$$

$\mathbf{M}$ does not depend on $\boldsymbol{\Theta}_S$ $\rightarrow$ signal and interference (clutter and noise) parameters are disjoint $\rightarrow$ CRB for $\boldsymbol{\Theta}_S$ same whether $\mathbf{M}$ is known or not.

Simulation Parameters

Radar parameters:

N_p	L	λ	PRI	Pos. of tx/rx subarray	range	θ	β
10	16	20 m	5 s	(0,0) m	70e3 m	0	2

Generation of clutter covariance matrix:

- Modeled by integration over azimuth angles, 180° (front lobe of receive subarray)
- Isotropic antenna elements
- Classical power budget equation for clutter with constant reflectivity
- CNR = 60 dB per element per pulse
- Estimated using $N_s = 500$ secondary data

Element distribution configuration:

Config	1	2	3	4
N	1	2	5	8
M	9	8	5	2

Element spacing configuration:

Config	a	b	c	d
α	1	2	1	2
γ	α	α	αM	αM

Detection Performance, Config 1-4, Adaptive (1/2)

T1 at $\omega_T = 0.01$ and T2 at $\omega_T = 0.2$

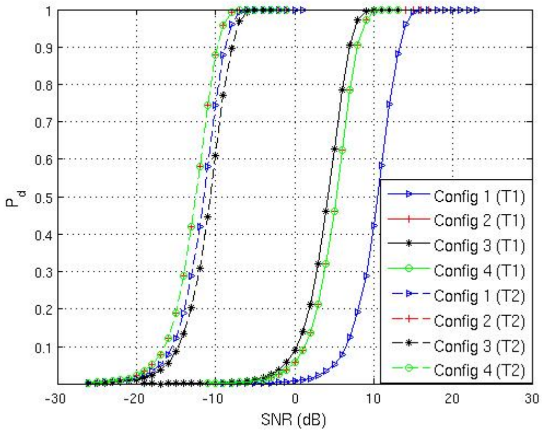

Detection Performance, Config 1-4, Adaptive (2/2)

Target T1:

- More important to have narrow clutter notch as target has low velocity
- MIMO configurations have larger $L_a \rightarrow$ smaller SIR loss for slow targets

Target T2:

- More important to have higher gain
- Config 3 also has largest $N_e \rightarrow$ largest SIR gain but also much loss from estimation of covariance matrix

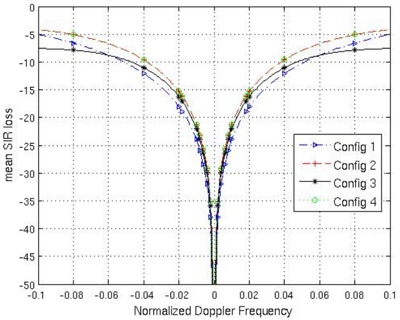

Config	N_s/MNL	$E(l_f)$ for $N_s = 500$
1	3.47	0.71
2	1.95	0.49
3	1.25	0.20
4	1.95	0.49

Detection Performance, Config a-d, Adaptive (1/2)

T1 at $\omega_T = 0.01$ and T2 at $\omega_T = 0.2$

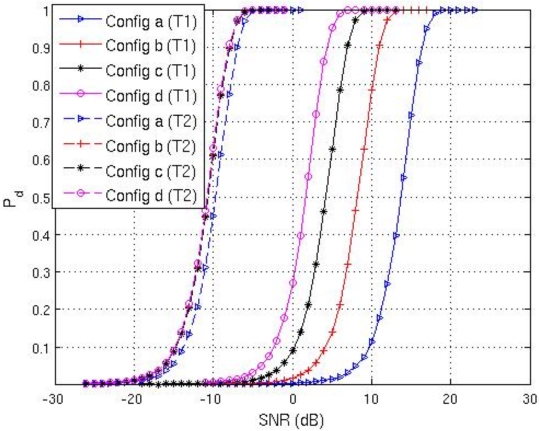

Detection Performance, Config a-d, Adaptive (2/2)

- Same *MNL* → same loss from estimation of covariance matrix → similar results for T2
- For T1, different detection performance due to different element spacing and resulting L_a

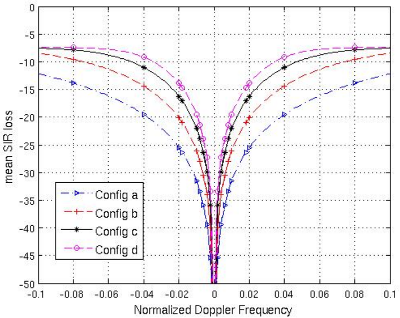

Config	N_s/MNL	$E(l)$ for $N_s = 500$
3	1.25	0.20

Estimation Performance, Config 1-4

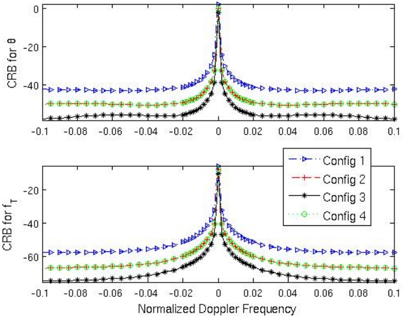

SNR = 10 dB

- Inter-element spacing according to Config c ($\alpha = 1$ and $\gamma = M$)
- CRB is low far from the clutter ridge, much higher at the clutter ridge ($f_T = 0$) due to strong clutter
- Config 3 gives the lowest CRB in general, i.e. better estimation accuracy. Its CRB peak is also the narrowest, indicating that it has the smallest MDV
- All the MIMO configurations (Config 2-4) better than classical STAP configuration (Config 1)

Estimation Performance, Config a-d

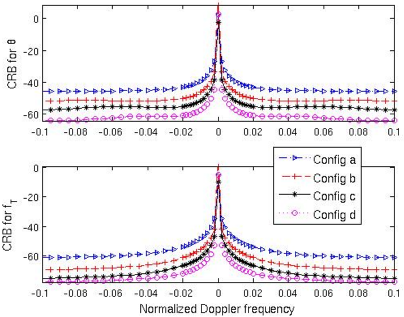

SNR = 10 dB

Config	ref	a	b	c	d
L_a/λ	4	4	8	12	21

- Classical STAP as reference
- Config a-d has equal no. of transmit and receive elements (Config 3) $\rightarrow$ maximizes SNR gain
- Config a has lower CRB than ref although they have the same L_a because of SNR gain
- Sparse config $\alpha > 1$ (config b and d) increases L_a further $\rightarrow$ lower CRB

MISO-STAP Signal Model

- Multiple widely separated transmit elements and one receive subarray
- Each tx-rx pair is in bistatic configuration and sees different target RCS, given by: $[a_1 e^{j\phi_1} \ \cdots \ a_{K_e} e^{j\phi_{K_e}}]$
- Different waveforms transmitted s.t. received signal can be separated

Received signal after range matched-filtering for the i-th subarray:

$$\begin{aligned} \mathbf{y}_i &= a_i e^{j\phi_i}\, \mathbf{a}(\theta_r) \otimes \mathbf{v}(f_{d,i}) + \mathbf{c}_i + \mathbf{n}_i, \\ &= a_i e^{j\phi_i}\, \mathbf{p}_i + \mathbf{c}_i + \mathbf{n}_i, \end{aligned}$$

where $\mathbf{p}_i$ is the space-time steering vector,
θ_r is the receive angle and $f_{d,i}$ is the relative Doppler frequency,
$\mathbf{c}_i \sim \mathcal{CN}(\mathbf{0}, \mathbf{M}_{c,i})$ is the clutter vector and $\mathbf{M}_{c,i}$ is the clutter cov matrix,
$\mathbf{n}_i \sim \mathcal{CN}(\mathbf{0}, \sigma^2\mathbf{I})$ is the noise vector and σ^2 is the noise power.

Simulation Parameters

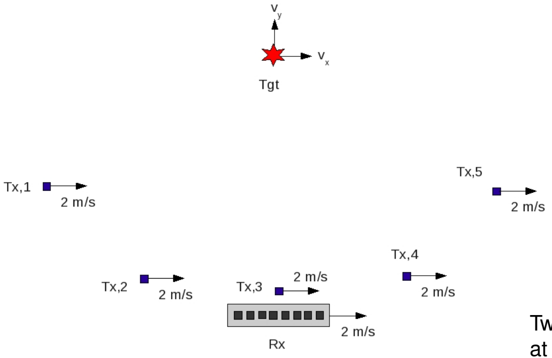

M	K_e	L	λ
8	1,2,5	16	20 m

PRI	θ	β	CNR
5 s	0	2	60 dB

Rx pos	Rx vel
(0,0)	(2,0) m/s

Tgt pos	Tx vel
(0,-70) km	(2,0) m/s

Tx x-pos	$70 \cdot \cos((-K_e : -1)\frac{\pi}{K_e+1})$ km
Tx y-pos	$70 \cdot \sin((-K_e : -1)\frac{\pi}{K_e+1})$ km

Two targets with random directions and at different absolute speeds:

0.1 m/s (T1) and 1.5 m/s (T2)

Detection Performance

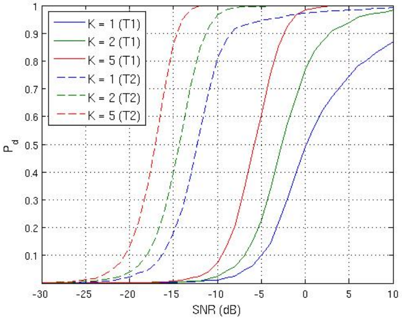

- $K_e = 1$ is classical STAP
- Better performance for larger K_e due to increased N_e and spatial diversity
- With spatial diversity $\rightarrow$ more robust to target fluctuations and changes in target velocity
- Due to diversity and geometry gains, detection curves for $K_e > 1$ converge to one fast

MISO Vs SISO

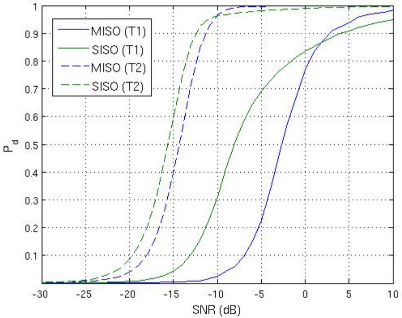

- Same number of elements for both configurations: $N_p = 10$ and $N_e = 16$
- SISO is better at low P_d because of improved resolutions
- MISO is better at high P_d due to its robustness against fluctuations of target RCS and velocity directions

Outline

Conclusions (1/4)

Gaussian Detector

- ◇ SIR gain depends on N_e which is maximized when equal number of transmit and receive elements irregardless of K_e,
- ◇ Larger K_e increases robustness against target fluctuations but also increases detection threshold,
- ◇ Configuration depends on application, e.g. small K_e for direction-finding and big K_e for surveillance,
- ◇ For estimation of covariance matrix, $N_s > 2N_e - 2K_e - 1$ for 3 dB loss

  $\Rightarrow$ for limited N_s, small N_e and large K_e to limit loss.

Conclusions (2/4)

Non-Gaussian Detector

- Homogeneous structure of the detector results in invariance to the texture characteristics $\Rightarrow$ texture-CFAR,
- Small CFAR loss under Gaussian interference and big improvements in performance under non-Gaussian interference $\Rightarrow$ more robust than the Gaussian detector.

Conclusions (3/4)

SISO-STAP

- Equal number of transmit and receive elements maximizes N_e and effective aperture size (for critical sampling) $\Rightarrow$ increase SIR gain and reduce MDV,
- Sparse configurations:
  - increase effective aperture size, reduce MDV and improve estimation accuracy,
  - do not cause additional ambiguity if spatial and Doppler ambiguities are matched,
  - reduce rank of CCM $\Rightarrow$ fewer secondary data required.

Conclusions (4/4)

MISO-STAP

- Can be easily achieved by adding single tx elements to existing STAP systems,
- Robust against target fluctuations and dependence of target velocity w.r.t. aspect angle,
- For the same number of elements (N_e and N_p), MISO config is better than SISO config at high P_d due to increased robustness; SISO better at low P_d due to improved resolution.

Future Works

- Signal Model
  - Include waveform and range information
  - Fluctuating models for target
  - Use of tensors for representation and calculations
- Target classification
- 2-step detection and estimation algorithm
- Validation with real data
- Low-rank methods for STAP
- Diagonal loading
- Estimation bounds

Thank you!